Sizing Approach with Flight Time Comparison of An Electric Multirotor Propulsion Chain with Batteries and Fuel Cells

Saad Chahba, Rabia Sehab, Guillaume Krebs, Ahmad Akrad, Cristina Morel

Sizing Approach with Flight Time Comparison of An Electric Multirotor Propulsion Chain with Batteries and Fuel Cells

Sizing Approach with Flight Time Comparison of An Electric Multirotor Propulsion Chain with Batteries and Fuel Cells

S Chahba[1*], R Sehab[1], G Krebs[2], A Akrad[1], C Morel[1]

[1]Pole Systèmes et Energies Embarqués pour les Transports S2ET, ESTACA Campus Ouest, Laval France.

[2]GeePs Group of electrical engineering-Paris, UMR CNRS 8507, CentraleSupélec, Université Paris-Saclay, Paris France.

[*]Corresponding author: Saad Chahba (email: saad.chahba@estaca.fr)

Abstract. The concept of electric vertical take-off and landing (E-VTOL) aerial vehicles is gaining more and more attention, thanks to their non-polluting operation and simple air traffic management. Indeed, around the world, there are currently more than 500 projects that concern the development and improvement of their performances. Development of sizing methods for rapid selection of the propulsion chain components remains an important task in this process. In this paper, an approach for sizing and selecting the propulsion chain components of an E-VTOL aerial vehicle is developed and validated. First, the optimal pair motor/propeller is selected using a global nonlinear optimization in order to maximize the specific efficiency of these components. Second, two energy storage technologies are considered and sized in order to assess their influence on the aerial vehicle flight time. Finally, based on this sizing process, the optimized propulsion chain gross take-off weight (GTOW) is evaluated, using regression methods based on propulsion chain supplier data.

1. Introduction

Traffic congestion is one of the main problems in big cities like Paris, London, New York, Copenhagen, and Delhi. The primary causes of it are high population, movement of people, and increase in private vehicles. In French metropolitan cities, such as Paris and Marseille, an average commuter loses every year over 80 hours in traffic resulting in an increase in stress and anxiety [1]. Such congestions also lead to 1.85 megatons per year of CO_2 emissions into the atmosphere. Besides having a detrimental impact on the health of the commuters and the environment, it also contributes to economic loss. Therefore, it is imperative to explore new modes of transportation to improve accessibility and mobility for passengers in urban areas and reduce traffic congestion.

The concept of electric vertical take-off and landing aerial vehicles (E-VTOL) represents one of the potential solutions to remedy this problem. Indeed, several aircraft manufacturers such as Airbus, Boeing, Lhilium, and Volocopter, have actively embarked on the development of this drone taxi technology in recent years [2]-[5]. E-VTOL aircraft are split into four main categories: Lift + Cruise, Tilt Rotor, Duced Vector Thrust and Multicopter. The first three categories go into the Powered lift aircraft category, which are winged aircraft capable of VTOL and aerodynamic lift in forward flight. The last one belongs to the wingless aircraft category. Multirotor aircraft is with two or more lift/thrust units with limited to no capabilities for wing borne forward flight. Powered lift e-VTOLs are further decomposed into two main categories, depending on whether the concept uses a common powerplant (Tilt Rotor and Ducted Vector Thrust) or independent powerplants (Lift + Cruise) for lifting and forward flight [6]-[8].

In this paper, we are interested in the urban air mobility (UAM) transport mode, in which the cruise phases are limited, so that the multirotor wingless configuration remains the best one for this transport market. One of the main steps in the E-VTOL design process, allowing to assess the adequacy of the proposed solutions, consists in sizing and choosing the components of the propulsion chain in order to meet the specifications. Therefore, sizing methodologies are needed to be developed for quick components choosing and constructing a new multicopter. Multirotor design methods have been

developed by Barshefsky [9], Dai [10] et Gur [11]. In [10] an analytical method to estimate the optimal parameters of the propulsion chain components is proposed, by describing the problem with mathematical expressions. Methodologies based on statistical data available from manufacturers for the preliminary design are reported in [11]. In this study, an approach for sizing and selecting the propulsion chain components is developed. This approach combines statistical methods based on data and analytical optimization techniques, which makes it possible to maintain an acceptable level of precision and avoid increasing the complexity of the calculation algorithm. In order to evaluate the effect of the energy storage element on the aerial vehicle range, two energy storage technologies are sized. The first is based on lithium polymer battery (LiPo) and the second is based on hydrogen fuel cell (PEMFC).
This paper is organized as follows. Section 2 is devoted to the presentation of the propulsion chain sizing algorithm, including the optimization technique used to select the optimal pair motor/propeller and the rest of the propulsion chain components. Section 3 presents the modeling of the propulsion chain components, in order to formulate the optimization problem allowing to maximize the pair motor/propeller specific efficiency. In section 4, the optimisation problem formulation is presented. Section 5 presents the sizing approach validation, using a reduced scale multirotor aerial vehicle of 15 kg. In section 6, conclusion is presented.

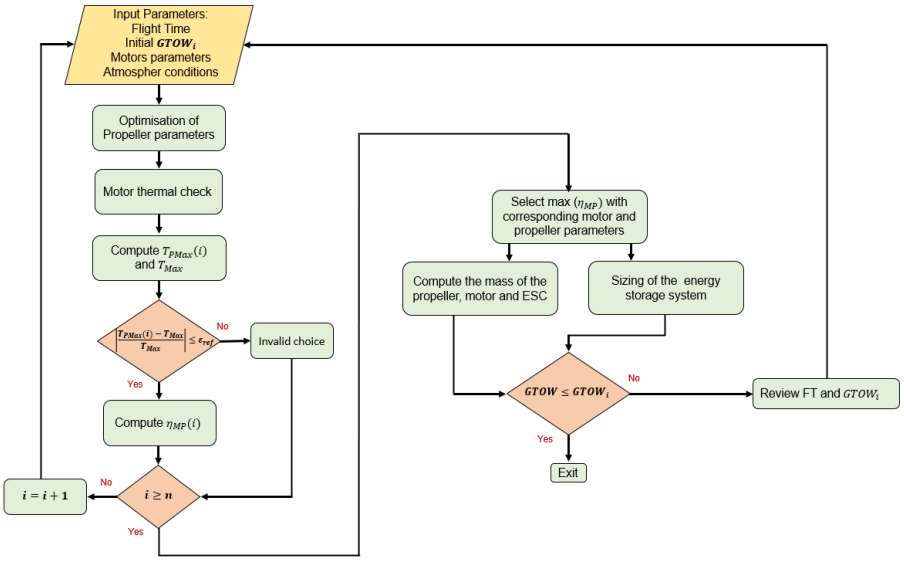

Figure 1: Sizing methodology for the E-VTOL multirotor flowchart

2. Sizing methodology

The sizing methodology is based on the combination of analytical optimisation techniques and data-based techniques. Figure 1 presents the flowchart of the sizing methodology.
First, the sizing methodology receives as inputs the required flight time, a database of electric motors parameters, at this stage the optimal motor is not known, the hover altitude, the atmospheric conditions namely the temperature, and the air density; and the gross take-off weight ($GTOW$).
Next, for each motor/propeller pair a global non-linear optimization, based on the simulated annealing algorithm (SAA), is performed. This optimization consists in maximizing the specific efficiency $\eta_{MP}(g/w)$, given in equation (10), which is an index widely used by industrials like T-motor[12] and Mejzlik[13], in order to measure the efficiency between the motor and the propeller, with constraints on the propeller geometry, one on the diameter in order to avoid motor overheating, this constraint is given in equation (12); and the other on the pitch angle which is imposed by the geometry.
Then, the obtained pair motor/propeller makes it possible to calculate the maximum thrust $T_{MP_{max}}$ given in equation (14). Using the maximum thrust T_{Max} imposed by $GTOW$, a filtering condition is established, in order to make an initial selection of the pairs propeller/motor.
After that, the selection of the optimal motor/propeller torque is conditioned by the maximum specific efficiency obtained. The sizing of the energy sources is carried out in such a way that the flight time is maximum.

Finally, the last step of this sizing methodology consists in verifying whether the total take-off mass, using the mass statistical models of each propulsion chain component based on supplier data, obtained is respected.

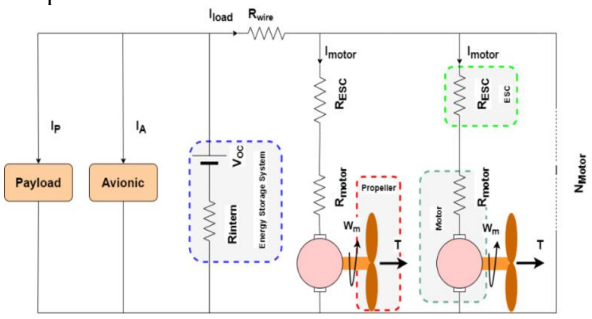

Figure 2: E-VTOL multirotor physical model

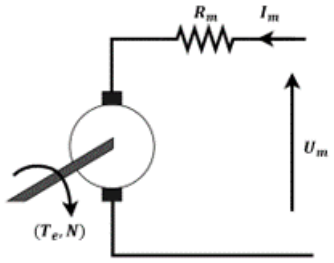

Figure 3: BLDC motor electric model

3. Propulsion chain modeling

The physical model of the propulsion chain, of an E-VTOL multirotor aerial vehicle, with n arms is presented in Figure 2. Each propulsion chain is composed of a propeller, a motor, an electronic speed controller (ESC) and an energy storage system. In this configuration (Figure 2), the energy storage system supplies the n propulsion chains. The modeling process will aim to establish a relationship between the propulsion chain components, especially between the propeller and the motor, wording the optimization problem. In this case, each component will be modeled in steady state.

3.1. Propeller model

The propeller model in static state is described by its thrust $T[N]$, and its torque $M[Nm]$ as given by equation (1) [14]:

$$T = C_T * \rho * \left(\frac{N}{60}\right)^2 * D_p^4 \qquad and \qquad M = C_M * \rho * \left(\frac{N}{60}\right)^2 * D_p^5 \tag{1}$$

where $\rho[kg/m^3]$, C_T , C_M, $N[rpm]$, and $D_p[m]$ are respectively, the air density, the thrust coefficient, the torque coefficient, the propeller velocity, and the propeller diameter. The air density ρ is determined by both the local temperature $T_t[°C]$ and the air pressure p, which is further determined by altitude $h_{hover}[m]$. The thrust and the torque coefficients are [15]:

$$C_T = \frac{0.27\pi^3\lambda\zeta^2 K_0\varepsilon}{\pi A + K_0} B_p^{\alpha_t}\varphi_p \qquad and \qquad C_M = \frac{1}{4A}\pi^2\lambda\zeta^2 B_p\left(C_{fd} + \frac{\pi A K_0^2\varepsilon^2}{e(\pi A + K_0)^2}\varphi_p^2\right) \tag{2}$$

where B_p and $\varphi_p[rad]$ are respectively the propeller blade number and the pitch angle. They are defined using: $\varphi_p = \arctan\left(\frac{H_p}{\pi \cdot D_p}\right)$. $A, \varepsilon, \lambda, \zeta, e, C_{fd}$ and K_0 are the blade parameters, which are directly related to the propeller blade airfoil shape. The carbon fiber blade parameters values are $A = 5, \varepsilon = 0.85, \lambda = 0.75, \zeta = 0.5, e = 0.83, C_{fd} = 0.015, \alpha_t = 0.9$ and $\rho = 1.2[kg/m^3]$. The figure 4 gives the regression model of the propeller mass $M_{prop}[g]$ based on data supplied. The input of this model is propeller diameter Dp. The regression model of the propeller mass is $M_{prop} = 0.303 \cdot D_p^4 - 9.729 \cdot D_p + 105.786$.

3.2. Electric motor model

In figure 3, $U_m[V]$ is the supply voltage, $I_m[A]$ is the current absorbed by the motor coils, $R_m[\Omega]$ is the motor equivalent resistance, $T_e[N \cdot m]$ is the electromotive torque produced by the motor, and $N[rpm]$ is its shaft angular velocity. The equations describing the motor electric model [16] are:

$$\begin{cases} U_m = e_a + R_m \cdot I_m \\ T_e = K_T \cdot I_m \\ E_a = K_E \cdot N \approx \dfrac{N}{K_v} \end{cases} \tag{3}$$

where $K_E[V \cdot s/rad]$ is the motor back EMF constant, $K_T\ [N \cdot m/A]$ is the motor torque constant, N is the motor rpm, and $K_v[rpm/V]$ is speed constant. The K_T and K_E are related to K_v by: $K_E = \frac{1}{K_v} = \frac{\pi}{30} \cdot$

K_T . The motor output torque and the propeller torque are related by: $M = T_e - T_0 = K_T \cdot (I_m - I_{m0})$. Using these equations and the first one, U_m and I_m are given as follow:

$$I_m = \frac{\pi}{30K_v} M + I_{m0} \qquad and \qquad U_m = I_m R_m + \frac{N}{K_v} \tag{4}$$

The mass regression model of the electric motor is given by the figure 5. The motor data used in this model are collected form [12] and [17], with the input, the motor speed constant K_v. The regression model of the motor mass is given by: $M_{mot} = 0.00048K_v^2 - 1.461K_v + 840.617$.

3.3. Electronic speed controller

In the developed sizing methodology, the ESC electric model is not considered. However, the ESC maximum continuous current I_{emax} must be fixed, especially for the selection and the mass estimation steps [18]. The figure 6 gives the mass regression model of the ESC based on supplier data; collected from T-motor and KDEDirect. The regression model of the ESC mass is given by: $M_{ESC} = 0.016I_{emax}^2 - 0.638I_{emax} + 42.414$.

3.4. Energy storage system

In this part, two energy sources are considered, the first one is a lithium polymer (Li-Po) battery, the second one is a proton membrane exchange (PME) hydrogen fuel cell.

3.4.1. Battery modeling Due to their high energy density and discharge rate, e-VTOLs use Li-Po batteries. Each Li-Po cell is defined with a nominal voltage of $3.7V$, a capacity $C_{cs}[Ah]$, and a power density of $\rho_b = 140[Wh/kg]$ [18]. The nominal voltage and the total battery capacity of Li-Po battery are respectively $U_b = 3.7 \cdot n_c$ and $C_b = n_p \cdot C_{cs}$, where n_c and n_p <are respectively the number of cellules connected in series and in parallel. The battery output power P_b can be estimated by $P_b = N_m \cdot P_m \cdot \eta_e \cdot \eta_b$, where N_m, η_e, and η_b are respectively the propulsion chain number, the conversion efficiency of ESC, and the battery efficiency. The flight time $t_{flight}[min]$ of the e-VTOL(battery time discharging) is $t_{flight} = \frac{60 \cdot \rho_b \cdot m_b}{P_b}$, where m_b, and P_b are respectively the battery mass (kg), and the battery power (W).

3.4.2. Hydrogen fuel cell modeling PEM fuel cells offer a higher energy density than batteries, around $500W\ h/kg$ [19], in a unit that is hydrocarbon free, mechanically simple, operates near ambient temperature, and produces no harmful emissions. In terms of fuel cell power density, there are several works estimating its improvement for a value of $800[W/kg]$ [19]. A PEM stack consists of identical cells each with a voltage $E_{cell}[V]$ [19]. The nominal voltage of a PEM stack and a cell area are given: $V_{stack} = N_{cell} \cdot E_{cell}$ and $A_{cell} = \frac{P_{FC}}{p_{cell} \cdot N_{cell}}$, where P_{FC}, p_{cell}, and N_{cell} are respectively the required electrical power, the power density of single cell, and the cell number. As well for the case of the battery, the fuel cell output power required for the flight mission P_{FC} and the corresponding hydrogen consumption $HC(kg/h)$ can be estimated by:

$$P_{FC} = N_m \cdot \frac{P_m}{\eta_e \cdot \eta_{FC}} \qquad and \qquad HC = \frac{P_{FC}}{LHV \cdot \eta_{FC}} \tag{5}$$

where $\boldsymbol{\eta_{FC}}$, and $\boldsymbol{LHV}$ are respectively the fuel cell stack efficiency, and the low heating value of hydrogen ($\boldsymbol{33.3Wh/g}$). At the current technology level, the efficiency of the PEMFC is approximately $\boldsymbol{40-50}$%. This value can be used for sizing if there is no information about the polarization curve of a single cell. Thus, the hydrogen fuel cell mass $\boldsymbol{m_{FC}}$ is given by [19]:

$$m_{FC} = \frac{N_{cell} \cdot k_A \cdot \rho_{cell} \cdot A_{cell}}{1 - \eta_{ow}} (1 + f_{BOP}) \tag{6}$$

Where $\boldsymbol{k_A}$, $\boldsymbol{\rho_{cell}}$, $\boldsymbol{f_{BOP}}$ and $\boldsymbol{\eta_{ow}}$ are respectively ratio of the cross-sectional area to the electrode area of a single cell, and it fixed at value of five, the area density of a single cell, and its value is fixed as $\boldsymbol{1.57kg/m}$; ratio of the $\boldsymbol{BOP}$ weight to the HFC weight, and its value is different depending on the HFC configuration, in this paper a value of 0.2 is considered; overhead fraction to account for gaskets, seals, connectors, and endplates; and it's fixed at 0.3. The flight time in the case of a fuel cell is given by the following expression:

$$t_{flight} = \frac{60 \cdot LHV}{P_{FC}} \tag{7}$$

A regression model that estimates the hydrogen tank mass $\boldsymbol{M_{tank}[kg]}$, based on the amount of hydrogen $\boldsymbol{m_{H_2}[g]}$ required for the flight mission, is established as shown in figure 7. The data are based on tank of type 3 and 4 [21], and this model can be expressed as: $\boldsymbol{M_{tank} = -0.000047 m_{H_2}^2 + 0.0367 m_{H_2} - 0.112}$.

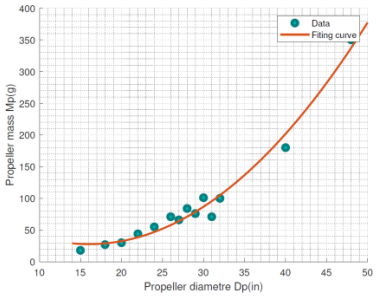

Figure 4: Regression model of the propeller mass,

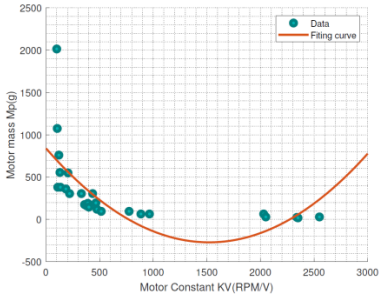

Figure 5: Regression model of the motor mass,

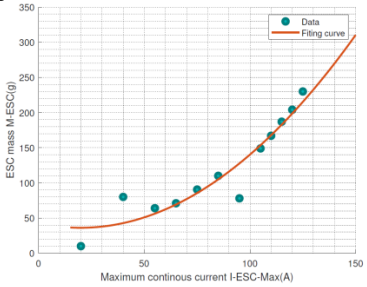

Figure 6: Regression model of the ESC mass,

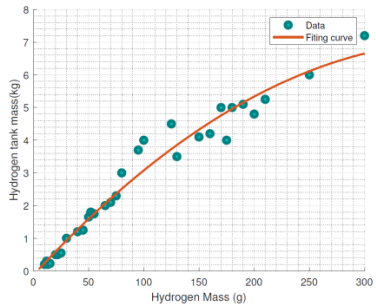

Figure 7: Regression model of the hydrogen tank mass.

4. Optimization problem

The optimization technique is based on simulated annealing algorithm (SAA), which was introduced by inspiring the annealing procedure of the metal working. In general manner, SA algorithm adopts an iterative movement according to the variable temperature parameter which imitates the annealing transaction of the metals [21]. This algorithm is directly explored using global optimization toolbox of MATLAB. The efficiency of the pair motor/propeller $\eta_{MP}[N/w]$, which is also called specific efficiency, is used as an objective function in this case. This function is $\eta_{MP} = \frac{t_{flight}}{P_{mflight}}$, where t_{flight} and $P_{mflight}$ are the propeller thrust and the motor power during the flight operation. From the propeller model presented in equation (1), the propeller velocity and the propeller torque during flight are given by:

$$N_{flight} = \frac{60}{D_p^2}\sqrt{\frac{T_{flight}}{\rho C_T}} \qquad and \qquad M_{flight} = \frac{C_M D_p}{C_T} T_{flight} \tag{8}$$

Using the motor model (4), the motor current and the motor voltage are:

$$\begin{cases} I_{m0} \approx 0 \\ I_{mflight} = \dfrac{\pi C_M D_p}{30 C_T K_E} T_{flight} \\ U_{mflight} = \dfrac{\pi C_M D_p}{30 C_T K_E} T_{flight} R_m + \dfrac{60 K_E}{D_p^2}\sqrt{\dfrac{T_{flight}}{\rho C_T}} \end{cases} \tag{9}$$

Thus, the function objective expression is given by:

$$\eta_{MP} = \frac{1}{\left(\frac{\pi C_M D_p}{30 C_T K_E}\right)^2 T_{flight} R_m + \frac{2\pi C_M}{D_p \sqrt{\rho C_T^3}} \sqrt{T_{flight}}} \tag{10}$$

For a fixed thrust imposed by the $GTOW$, the motor/propeller efficiency evolution in terms of propeller parameters is given in the figure 8. Through this figure, it's noticeable that the motor/propeller efficiency presents a single attraction basin, which allows to rapidly locate the point maximising the function objective. In order to avoid the motor overheating during the flight, which could influence on the efficiency, the motor current and voltage must remain below their maximum values imposed by the motor design: $U_m \leq U_{mMax}$ and $I_m \leq I_{mMax}$, which leads to establish constraint on the propeller velocity and torque:

$$N_{max} = \frac{(U_{mMax} - R_m \cdot I_{mMax})}{K_E} \qquad and \qquad M_{max} = \frac{30 \cdot (I_{mMax} - I_{m0}) K_E}{\pi} \tag{11}$$

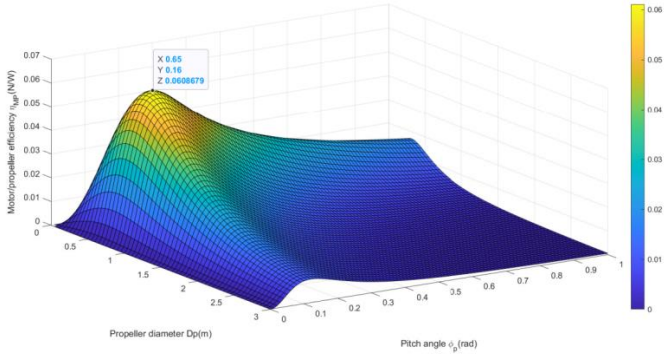

Figure 8: Motor/propeller efficiency in terms of propeller parameters.

Thus, the propeller diameter must remain below of its maximum value D_{pMax} imposed by the motor overheating avoidance condition:

$$D_p \leq D_{pMax} = \sqrt[5]{M_{max} \cdot \left(\frac{60}{N_{max}}\right)^2 \cdot \frac{1}{C_M \rho}} \tag{12}$$

The optimisation problem of the motor/propeller is given as follows:

$$\begin{cases} max(\eta_{MP}) = min(-\eta_{MP}) \\ 0 < D_p \leq D_{pMaxElec} \\ 0 < \varphi_p \leq \pi \end{cases} \tag{13}$$

5. Sizing approach validation

The validation of the proposed sizing approach is carried out using multirotor drone data (table 1) of figure 9, with a $GTOW$ of $15\,kg$. It is composed of 8 propulsion chains, with motor type $U7 - V\ 2.0\ 420K_V$, and propeller type $P18x6.1$. Each 4 propulsion chains are supplied by one $6S1P$ LiPo battery. A simulation of the propulsion chain sizing approach is carried out using MATLAB, and an electric motors parameters data base of 45 examples.

Figure 9: Multirotor drone,

Table 1. Multirotor drone specifications.

Component	Parameters
Propeller	$D_p = 18in;\ H_p = 6;\ \varphi_p = 1.336\ rad$
Motor	$KV = 420;\ U_m = 22.2V;\ I_m = 35A;\ R_m = 0.071\Omega$
ESC	$I_{ESCMaxm} = 35A$
Battery	$U_b = 22.2V;\ C_b = 12Ah;\ C - rate\ 30C$
Fuselage	$M_F = 5kg$
Load	$M_L = 3kg$

5.1. Pair motor/propeller optimization

The filtering condition is based on the computing of the relative error ε_r, given by: $\varepsilon_r = \left|\frac{T_{MP_{max}} - T_{Max}}{T_{Max}}\right|$, between the maximum thrust $T_{MP_{max}}[N]$ generated by the optimised pair motor/propeller and the thrust imposed by the $GTOW$, $T_{max}[N]$. The maximum thrust generated by the optimised pair motor/propeller is given by:

$$T_{MP_{max}} = \sqrt[5]{M_{max}^4 \cdot \frac{C_T^5}{C_M^4} \cdot \left(\frac{N_{max}}{60}\right)^2} \tag{14}$$

The thrust imposed by the drone $GTOW$ is deduced from the acceleration a_c required during the flight: $T_{Max} = \frac{GTOW \cdot (g + a_c)}{N_p}$, where g and N_p are receptively the gravity acceleration and propulsion chain number. An error reference value $\varepsilon_{ref} = 5\%$ is fixed as threshold value in order to make the filtering process. The motor/propeller combinations which are able to generate the thrust imposed by the specifications are given by table 2. It is remarkable that the two combinations in terms of the specific efficiency η_{MP} remain equivalent, which makes the choice between them very similar. The combination 1 is used in the considered drone for the validation.

Table 2: Sizing process methodology outcome,

Combination number	Motor specification	Propeller parameters	Thrust efficiency
1	$U7 - V2.0\ KV420$	$P18x6.0$	$0.0528\ (N/W)$
2	$U7 - V2.0\ KV490$	$P20x6.7$	$0.0528\ (N/W)$

Table 3: Mass evaluation of the propulsion chain components.

Component	Propeller	Motor	ESC	Battery	Fuel cell stack	Hydrogen tank	Hydrogen
Mass(kg)	0.0395	0.3071	0.0482	6.58	4.1825	2.3204	0.077

5.2. Energy storage sizing and flight time comparison

The sizing of the storage energy system is based on the maximisation of the flight time by keeping the $GTOW$ as minimal as possible. After the optimal motor/propeller pair has been selected by the optimization algorithm, the sizing of the ESC part will be conditioned by the maximum current imposed by the motor. The fuselage dimensioning part is not considered in this paper, it is assumed that it is ready. The drone mass is estimated as: $m_{copter} = m_{storageEnergy} + m_{others}$.

- Battery sizing: from the discharging time of battery, the drone flight time is related to the motor/propeller efficiency by:

$$t_{flight} = \frac{\eta_e \cdot \eta_b \cdot \rho_b \cdot m_{bat}}{(m_{bat} + m_{others}) \cdot g} \cdot \eta_{MP} \tag{15}$$

- HFC sizing: from the discharging time in the HFC case, the drone flight time is related to the motor/propeller efficiency by:

$$t_{flight} = \frac{\eta_e \cdot \eta_{FC} \cdot LHV \cdot m_{H_2}}{(m_{STACK} + m_{others}) \cdot g} \cdot \eta_{MP} \tag{16}$$

where m_{STACK} is the stack fuel cell mass, which is given by: $m_{STACK} = m_{FC} + m_{H_2} + m_{tank}$.

A simulation is carried out based on validation drone data given in table 1. By fixing other parameters and varying the battery mass or the hydrogen mass; the evolutions of flight time in term of the battery mass or the hydrogen mass are given in figure 10(a-b). It's observable, for both cases, that the flight time increases at first, and then decreases as the battery mass or the hydrogen mass increases from 0 to ∞. The decreasing of the flight time is caused by the decreasing of the thrust efficiency when the drone weight is too heavy. Usually, the flight time maximum is not reached, because the energy storage system mass is limited by the $GTOW$. Thus, the optimum weight of the battery must be sought in the permitted region given in figure 10(a-b). The optimised parameters of the hydrogen fuel cell are: $N_{cell} = 32$, $A_{cell} = 0.0486\ m^2$ and $V_{FC} = 22.2V$. Once the battery mass is calculated, the battery capacity is

given by: $C_b = \frac{m_{bat} \cdot \rho_b}{U_b}$. Based on the regression model of each component, a mass estimation of the propulsion chain is given in table 3. The fuselage mass and load mass are given in table 1. The optimised gross take-of weight is given by $GTOW = 14,9747kg$.

It is remarkable that the hydrogen fuel cell allowed to have an autonomy of 30 min, in comparison with the battery which allowed only 14 min of autonomy, that is to say half compared to the hydrogen cell (Figure 11). Indeed, the hydrogen fuel cell remains the best solution for long-flight missions at low altitudes

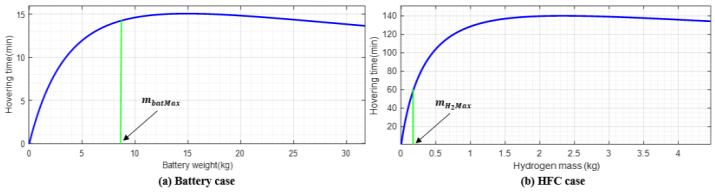

Figure 10: Flight time evolution,

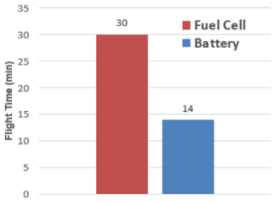

Figure 11: Flight time comparison.

6. Conclusion

In this paper a sizing methodology is presented and developed for propulsion chains used in e-VTOLs. This methodology is based on analytical design, used to select the optimal motor/propeller pair, and statistical technics in order to estimate the $GTOW$. Its main advantages reside in its high accuracy, very fast computing time and simple to implement. The comparison between two energy sources, namely a LiPo battery and a PEM hydrogen fuel cell, has shown the interest of hydrogen fuel cells for this type of aeronautical application. However, some perspectives are suggested, especially the extension of the validation step to real scale examples, and the consideration of a hybrid energy storage structure with battery and fuel cell or supercapacitor and fuel cell in order to improve the reliability and to maximise the range for a flight mission.

References

[1] TomTom Traffic Index. Available online: https://www.tomtom.com/en-gb/traffic-index/ranking/
[2] Airbus city project. Available online: https://www.airbus.com/en/innovation/zero-emission/urban-air-mobility/cityairbus-nextgen
[3] Boeing Passenger Air Vehicle. Available online: https:// www.boeing.com/features/frontiers /2019/autonomous-flying-vehicles/index.
[4] Lilium Jet. Available online: https://lilium.com/jet
[5] Volocopter UAM. Available online: https://www.volocopter.com/urban-air-mobility/
[6] Nathen P, Andreas S, R. Miller, S. Grimshaw and J. Taylor. “Architectural performance assessment of an electric vertical take-off and landing (e-VTOL) aircraft based on a ducted vectored thrust concept.” (2021).
[7] Doo J- T., Pavel M-D, Didey A, Hange C, Diller N-P, Tsairides, M. A., Smith, M., Bennet, E., Bromfield, M., and Mooberry, J. ”NASA Electric Vertical Takeoff and Landing (eVTOL) Aircraft Technology for Public Services – A White Paper,” NASA Transformative Vertical Flight Working Group 4 (TVF4). National Aeronautics and Space Administration, Washington, D.C., 2021.
[8] Ugwueze O, Horri T, Innocente N, Bromfield M. (2022). Investigation of a Mission-based Sizing Method for Electric VTOL Aircraft Preliminary Design. 10.2514/6.2022-1931.
[9] Bershadsky D, Haviland S, Johnson E N. (2016). Electric Multirotor UAV Propulsion System Sizing for Performance Prediction and Design Optimization.
[10] Dai X, Quan Q, Ren J, and Cai K-Y, ”An Analytical Design-Optimization Method for Electric Propulsion Systems of Multicopter UAVs With Desired Hovering Endurance,” in IEEE/ASME Transactions on Mechatronics, vol. 24, no. 1, pp. 228-239, Feb 2019.
[11] Gur O, Rosen A, 10-12 September 2008,” Optimizing Electric Propulsion Systems for UAVs,” AIAA 2008- 5916. 12th AIAA/ISSMO Multidisciplinary Analysis and Optimization Conference 1em plus 0.5em minus 0.4em Victoria, British Columbia Canada.
[12] T-motor. Available online on : https://store.tmotor.com/goods.php?id=384.
[13] Mejzlik. Available online on: https://www.mejzlik.eu/technical-data/propeller-data
[14] Ampatis C, and Papadopoulos E.” Parametric design and optimization of multi-rotor aerial vehicles,” 2014 IEEE International Conference on Robotics and Automation (ICRA), 2014, pp. 6266-6271.
[15] Brandt J and Selig M, Propeller Performance Data at Low Reynolds Numbers, 49th AIAA Aerospace Sciences Meeting, AIAA 2011-1255. 2011.
[16] Harrington A-M, Kroninger C. Characterization of Small DC Brushed and Brushless Motors, Aberdeen Proving Ground, USA, 2013.
[17] KDEDirect. Available online on: https://www.kdedirect.com/collections/uas-multi-rotor-brushless-motors
[18] Aurbach D, Gofer Y, Lu Z, Schechter A, Chusid O, Gizbar H, and Levi E. A short review on the comparison between Li battery systems and rechargeable magnesium battery technology. J. Power Sources 2001.
[19] Ng W, Datta A.” Hydrogen Fuel Cells and Batteries for Electric-Vertical Takeoff and Landing Aircraft”. Journal of Aircraft 2019. 1765-1782.
[20] Intelligent Energy. Available online: https://www.intelligent-energy.com/
[21] Yavuz Eren, ˙Ibrahim B. K¨u¸c¨ukdemiral, ˙Ilker Usto˘glu, Chapter 2 - Introduction to Optimization, Optimization ¨ in Renewable Energy Systems, Butterworth-Heinemann, 2017, Pages 27-74